ISSN 0023-1584, Kinetics and Catalysis, 2012, Vol. 53, No. 4, pp. 440–448. © Pleiades Publishing, Ltd., 2012.
Original Russian Text © E.V. Korneeva, A.S. Ivanova, D.A. Zyuzin, E.M. Moroz, O.A. Stonkus, V.I. Zaikovskii, I.G. Danilova, 2012, published in Kinetika i Kataliz, 2012, Vol. 53, No. 4, pp. 461–469.

Effect of Surfactants on the Structure and Texture Characteristics of Aluminum Oxide

E. V. Korneeva, A. S. Ivanova, D. A. Zyuzin, E. M. Moroz, O. A. Stonkus, V. I. Zaikovskii, and I. G. Danilova

Boreskov Institute of Catalysis, Siberian Branch, Russian Academy of Sciences, Novosibirsk, 630090 Russia
e-mail: kulko@catalysis.ru

Received November 30, 2011

Abstract—The effect of surfactants (polyvinyl alcohol and cetyltrimethylammonium bromide), which were introduced at the aluminum hydroxide synthesis stage, on the structure and texture characteristics of aluminum oxide was studied by a set of physicochemical techniques. The introduction of the above surfactants did not cause considerable changes in the thermal transformations of aluminum hydroxides, but it affected the genesis of the formed carbon. An analysis of the diffuse reflectance spectra and electron micrographs indicated that the aluminum oxide obtained in the presence of polyvinyl alcohol and calcined at 300°C was covered with polyene-type coke. An increase in the treatment temperature to 550°C led to the formation of condensed aromatic coke; in this case, the specific surface area of the sample increased from 125 to 500 m^2/g. The samples calcined at 550°C were γ-Al_2O_3 with a unit cell parameter of 7.933 Å and a crystallite size of no more than 30–40 Å. The pore size distribution was bimodal, with maximums at 35–65 and 380–415 Å, regardless of treatment temperature.

DOI: 10.1134/S0023158412040040

INTRODUCTION

Aluminum oxide in its γ modification has been widely used as a support, catalyst, adsorbent, etc., in various processes. Certain requirements are imposed on aluminum oxide in terms of phase composition, texture, and morphology, depending on its intended use; however, as a rule, its uncontrollable porosity restricts the application of this material. In particular, it is desirable to use alumina supports with a large pore volume and a narrow pore size distribution in the preparation of catalysts for the conversion of heavy petroleum fractions. Recently, attention has been focused on the synthesis of mesoporous oxide materials with a large specific surface area and a specified pore size distribution.

Mesoporous materials are prepared by the thermal treatment of mesostructured surfactant-templated precursors. The template approach was used in the synthesis of different mesoporous metal oxides, including titanium oxide [1] and zirconium oxide [2]. In spite of increased interest in mesoporous aluminum oxides [3, 4], studies in this area are scanty. The first example of the preparation of mesoporous materials based on aluminum oxide, including Al^{3+} cations and anionic surfactants such as alkyl sulfonates or phosphates, was reported by Huo et al. [5]; however, they prepared only lamellar, thermally unstable mesophases by this method. More recently, information on the preparation of aluminum-based dodecyl sulfate mesophases with a hexagonal structure under morphological control has been published [6, 7]. They were prepared by homogeneous precipitation, slowly increasing pH by the decomposition of urea. The layered material that formed at a low pH, was subsequently converted into a hexagonal phase at a higher pH. Various morphological forms appeared, depending on the concentration of urea; however, amorphous aluminum oxide with a specific surface area (S_{BET}) of 93 to 365 m^2/g and a pore volume of 0.4 cm^3/g was obtained after their thermal treatment.

Valange et al. [8] described the synthesis of mesoporous aluminum oxides by the formation of the Al-containing monomer $Al(H_2O)_6^{3+}$, oligomer complexes, or Keggin-type $[AlO_4Al_{12}(OH)_{24}(H_2O)_{12}]^{7+}$ cations in acidic solutions. These mesoporous mesophase aluminum oxides had specific surface areas from 300 to 820 m^2/g and mean pore diameters from 8 to 60 Å, depending on synthesis conditions.

Thus, the texture characteristics of aluminum oxide can be regulated by either changing the synthesis conditions or introducing a surfactant at the stage of the precipitation of the parent aluminum hydroxide [9, 10]. Here, we the influence of the nature and concentration of the surfactant and aluminum hydroxide precipitation and aging conditions on the structure and texture characteristics of the resulting aluminum oxide.

EXPERIMENTAL

Synthesis

Aluminum hydroxide was prepared by precipitation from a solution of aluminum nitrate with an aque-

Table 1. Conditions of the synthesis of aluminum hydroxides

Sample	Synthesis conditions*				
	surfactant	surfactant concentration, wt %	temperature, °C		aging time, h
			precipitation	aging	
A-1	–	–	30	90	3
A-2	CTAB	40	–/–	90	3
A-3	PVA	40	–/–	90	3
A-4	PVA	10	–/–	90	3
A-5	CTAB	40	–/–	110	72
A-6	PVA	40	–/–	110	72
A-7	PVA	10	–/–	110	24
A-8	PVA	10	–/–	110	120
A-9	PVA	10	–/–	70	3
A-10	PVA	10	70	70	3

* Both precipitation and aging were performed at pH 7.

ous solution of ammonium hydrocarbonate (NH_4HCO_3, $\rho = 1.055–1.064$ g/cm^3) in the presence of a surfactant. Cetyltrimethylammonium bromide (CTAB) and polyvinyl alcohol (PVA 7/2) at a concentration of 10 or 40 wt % were used as surfactants. Precipitation was performed at a constant pH 7.0–7.2 and a temperature of 30 or 70°C, followed by the aging of the suspension. Aging was performed at 70 to 110°C for 3–120 h. Then, the suspension was filtered, and the solid was washed with distilled water. The filtered sediment was dried in air and then in a drying oven at 120°C for 16–18 h. Table 1 specifies the synthesis conditions. The dried samples were calcined at 550–1100°C for 4 h.

Physicochemical Characterization Methods

Thermal analysis. Thermal analysis was carried out on a NETZSCH STA 449C system in the temperature range from 20 to 1000°C at a heating rate of 10 K/min in air. The sample weight was 0.1 g, and the weight loss was determined to within ±0.1%.

X-ray diffraction. The X-ray diffraction patterns were obtained on an HZG-4C diffractometer using radiation with a wavelength of 1.54184 Å and point-by-point scanning. Scanning was performed in the range of 10°–75° with a scanning step of 0.1°; the counting time per point was 5 s. Phase analysis was carried out by comparing the calculated values of interplanar spacing d and the corresponding diffraction peak intensity I with theoretical values from the PDF-2 database (ICDD). The sizes of coherent scattering domains (CSDs) were determined using the Selyakov–Scherrer formula from the integrated half-widths of the 4.4.0 diffraction peaks of the spinel structures of aluminum oxide. The unit cell parameter (a) of aluminum oxide was determined to within ±0.005 Å.

The diffraction patterns of a number of samples were obtained at the Precision Diffractometry and Anomalous Scattering Station of the Siberian Synchrotron and Terahertz Radiation Center (Budker Institute of Nuclear Physics, Siberian Branch, Russian Academy of Sciences). The diffraction beam of a Si(1.1.1) monochromator crystal with the degree of monochromation $\Delta\lambda/\lambda \approx 10^{-4}$ at the wavelength $\lambda = 0.699$ Å was used. The use of a powerful synchrotron radiation source not only shortened the exposure time but also increased the accuracy of analysis.

Electron microscopy. Electron microscopic studies were performed on a JEM-2010 transmission electron microscope (JEOL) (resolution, 0.14 nm; accelerating voltage, 200 kV). Local energy-dispersive X-ray microanalysis (EDX), which was performed on an EDAX spectrometer (EDAX Co.), was used for determining the concentrations of elements and their concentration ratios. The samples were applied to a carbon substrate fixed on copper gauze.

Diffuse reflectance spectra. Diffuse reflectance ultraviolet and visible spectra in air were recorded on a UV-2501 PC spectrometer (Shimadzu) in the spectral region of 11000–54000 cm^{-1} using an IRS-250A diffuse reflectance attachment. The samples as powders were placed in a quartz cell with an optical path of 2 mm. The experimentally found sample reflection coefficients (R) were converted into the Kubelka–Munk units according to the equation $F(R) = (1-R)^2/2R$ [11]. The wavelength of light in diffuse reflectance spectroscopy (200–900 nm) considerably exceeded the particle size of the samples (<100 nm); this made it possible to average electronic properties over the entire particle volume.

Texture characteristics. The texture characteristics of the samples were determined using an ASAP-2400 Micromeritics instrument from isotherms of low-temperature (–196°C) nitrogen adsorption. The samples

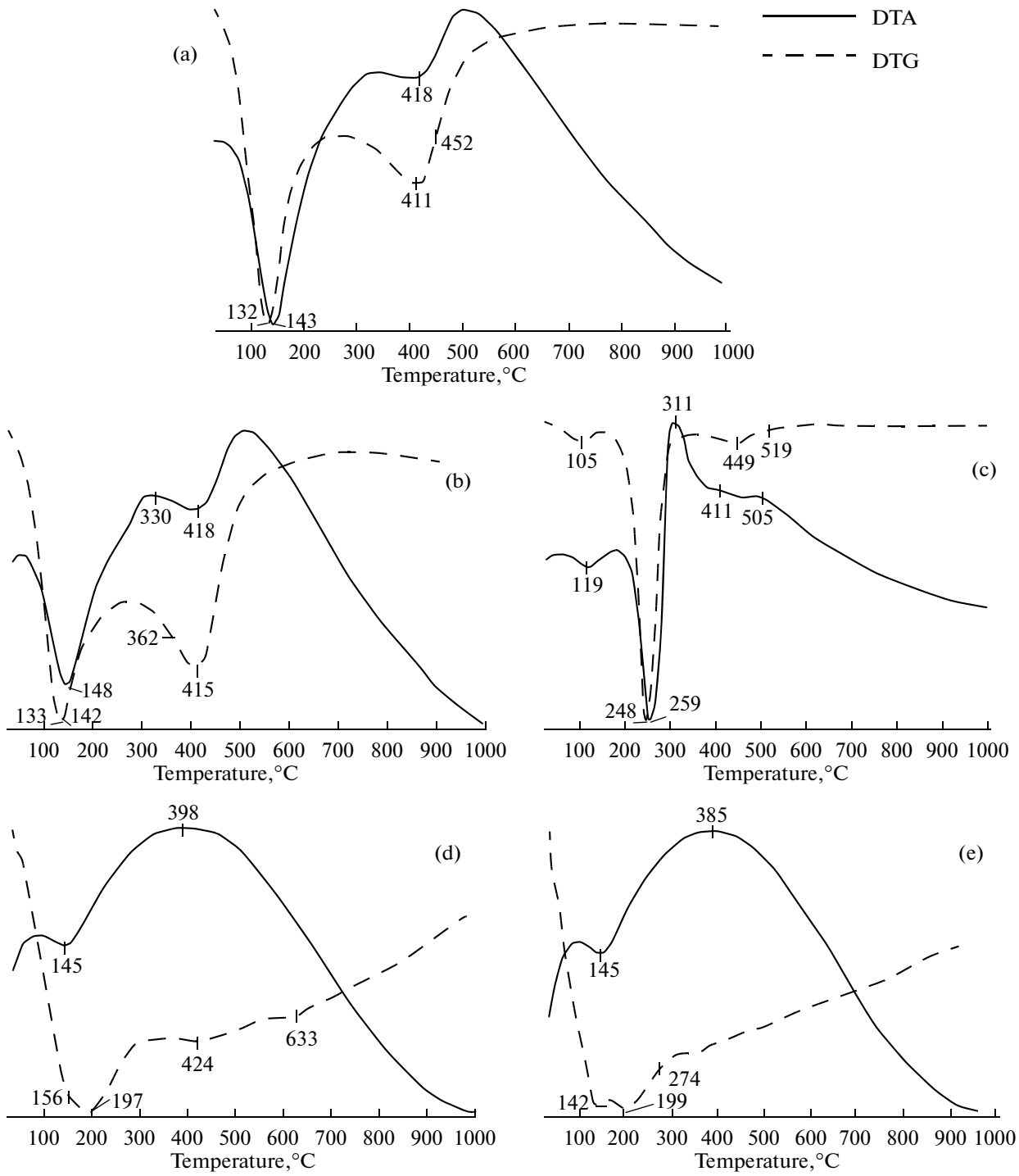

Fig. 1. DTA and DTG curves for samples (a) A-1, (b) A-2, (c) A-5, (d) A-3, and (e) A-6.

were preliminarily kept in a vacuum at 150°C; the error of the method was ±10%.

RESULTS AND DISCUSSION

Figure 1 shows the thermoanalytical curvess of samples A-1, A-2, A-3, A-5, and A-6, which differed in the nature of introduced surfactants and in the synthesis conditions. Sample A-1, which was prepared in the absence of a surfactant, was used for comparative characterization. The DTA curves exhibited endotherms and exotherma. The endotherm in the curve of reference sample A-1 at 132–143°C was caused by the removal of the physically adsorbed (free) water,

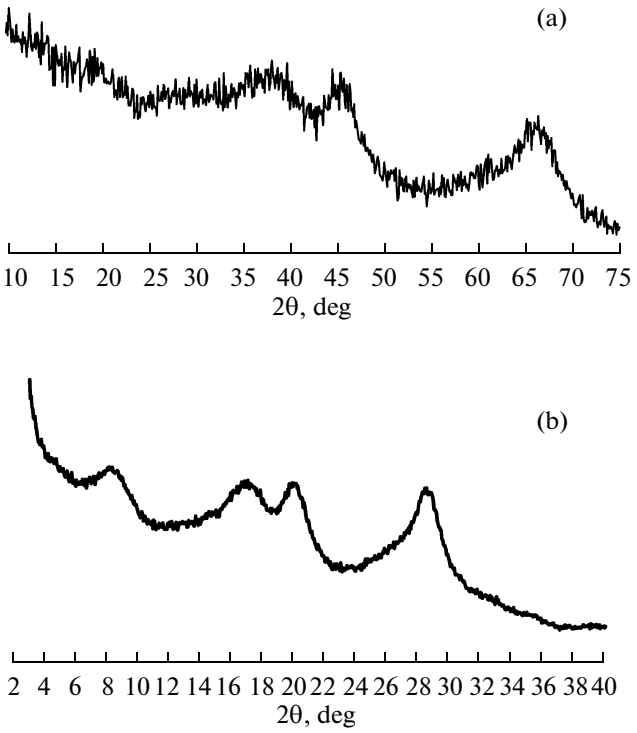

Fig. 2. Diffraction patterns of sample A-7 calcined at 300°C measured on (a) an HZG-4C diffractometer and (b) a high-resolution diffractometer at the Siberian Synchrotron and Terahertz Radiation Center.

whereas the endotherm at 411–418°C was due to the dehydration of pseudoboehmite with the formation of γ-Al_2O_3 (Fig. 1a) [12].

According to thermal analysis data, the introduction of surfactants (CTAB and PVA) at the aluminum hydroxide synthesis stage (samples A-2, A-5, A-3, and A-6) did not exert a considerable effect on the thermal transformations of the samples. The endotherms characteristic of the removal of free water (133–148°C) and the dehydration of pseudoboehmite with the formation of γ-aluminum oxide (415–418°C) were also observed for sample A-2 (Fig. 1b), which was prepared in the presence of 40% CTAB at 90°C. The thermoanalytical features in the region of 330–362°C can be attributed to the decomposition of CTAB; this is consistent with published data [13]. The thermal behavior of sample A-5, which was obtained in the presence of 40% CTAB but aged at 110°C for 72 h, was somewhat different (Fig. 1c): the removal of physically adsorbed water occurred at lower temperatures (105–119°C), and the endotherm due to the dehydration of pseudoboehmite was shifted to higher temperatures (449°C); this can be due to the formation of a better crystallized product [14]. Furthermore, an endotherm at 248–311°C was observed, which might also be due to the decomposition of CTAB (whose melting point is 250°C) [13].

Figures 1d and 1e show the thermoanalytical curves of the samples obtained in the presence of 40% PVA at aging temperatures of 90 and 110°C and aging times of 3 and 72 h (A-3 and A-6, respectively). Endotherms due to the removal of free water (142–156°C) were also characteristic of these samples. It is likely that the thermoanalytical features at 197–199°C were due to the decomposition of PVA, which occurs at 170–230°C [15, 16], and those at 385–398°C were due to the oxidation of residual PVA.

Thus, the introduction of surfactants did not exert a considerable effect on the thermal transformations of the resulting aluminum hydroxides. However, a change in aging conditions, in particular, an increase in aging temperature and time, in the presence of CTAB resulted in the appearance of an additional endotherm shifted to higher temperatures.

Because the introduction of PVA at the aluminum hydroxide synthesis stage and the aging conditions had almost no effect on the thermal genesis of the sample, we studied the phase composition of sample A-7, which was synthesized with the use of 10% PVA and

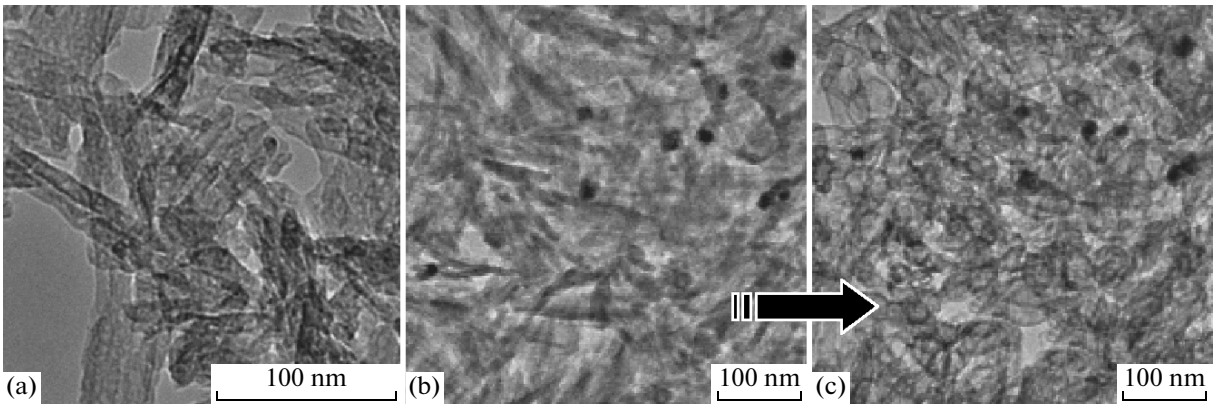

Fig. 3. (a) Particle morphology of sample A-7 dried at 110°C and TEM images of the same region of the sample (b) before and (c) after in situ heating with an electron beam.

Table 2. Phase composition and structure characteristics of sample A-7 calcined at different temperatures

Calcination temperature, °C	Phase composition			S_{BET}, m^2/g
	phase	a, Å	CSD, Å	
110	X-ray amorphous	–	–	125
300	X-ray amorphous	–	–	545
550	γ-Al_2O_3	7.933	30	500

was aged for 24 h at 110°C. According to X-ray diffraction data, sample A-7 dried at 110°C was X-ray amorphous (Table 2), as well as this sample calcined at 300°C (Table 2, Fig. 2a). Use of synchrotron radiation made it possible to obtain a higher quality spectrum (Fig. 2b) with a better ratio between peak intensities and background signals. In Fig. 2b, it can be seen that test sample A-7 contained an X-ray amorphous and poorly crystallized phase of γ-Al_2O_3 with a pseudospinel structure with cations distributed in the tetrahedral and octahedral holes of the close packing of oxygen, a portion of which was replaced by OH^- groups mainly on the surface [17]. The unit cell parameter of γ-Al_2O_3 was $a = 7.97$ Å, and the CSD size did not exceed 20 Å.

The small crystallite size of the resuilting oxide was consistent with the specific surface area of this sample, which was 545 m^2/g, whereas it was much smaller and did not exceed 125 m^2/g for the sample dried at 110°C (Table 2).

Sample A-7 calcined at 550°C was γ-Al_2O_3, whose unit cell parameter was 7.933 Å (Table 2), which is also larger than the tabulated value (7.911 Å [17]). Because the size of γ-Al_2O_3 crystallites was no greater than 30 Å, we can conclude that, in the presence of PVA, a fine particle oxide was formed; for this reason, the value of parameter a was larger and the specific surface area was greater (500 m^2/g, Table 2).

To reveal the cause of the formation of aluminum oxide with a high specific surface area (500–545 m^2/g), we performed an electron microscopic study of sample A-7 and recorded diffuse reflectance spectra.

According to electron microscopic data, the particles of sample A-7 dried at 110°C had a shape of slightly flattened needles 50–150 nm in length and 7–20 nm in width (on average, 70 and 10 nm, respectively) (Fig. 3a). The EDX spectra indicated the presence of carbon in the sample, whose average concentration was about 20 at % (in some areas of size ~100 nm, it was as high as 50 at % as a result of a nonuniform distribution). The presence of carbon was explained by the use of PVA in the synthesis of the samples.

The sample may heat as its electron micrograph is obtained; in order to evaluate this effect, we irradiated sample A-7, which was synthesized in the presence of PVA, with an electron beam in situ in the microscope. We found that the external dimensions of the needle-shaped particles and their aggregates did not change as a result of heating; however, the structure of the sample became defective. This manifested itself as a distortion of the needle shape of particles because of the appearance of surface roughness (Figs. 3b, 3c).

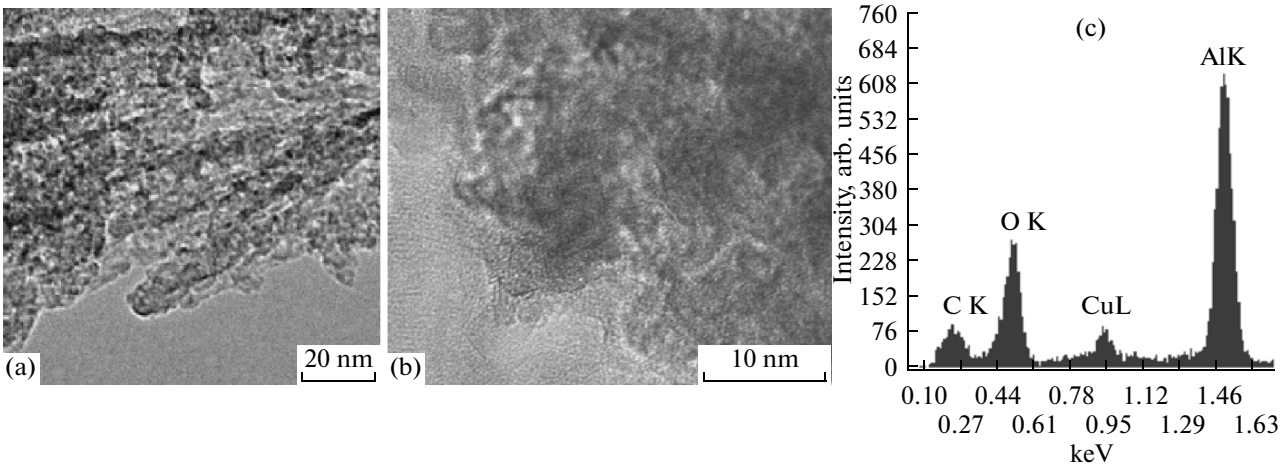

Fig. 4. (a) Defective particles of sample A-7 calcined at 300°C; (b) disordered Al_2O_3 structure at the particle edge; and (c) the EDX spectrum of a sample particle.

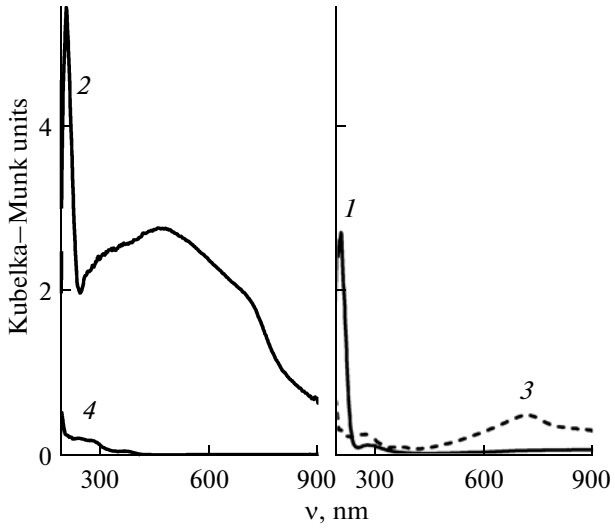

Fig. 5. Diffuse reflectance spectra of sample A-7 prepared in the presence of PVA and calcined at (*1*) 110, (*2*) 300, or (*3*) 550°C and (*4*) aluminum oxide synthesized with no surfactant and calcined at 550°C.

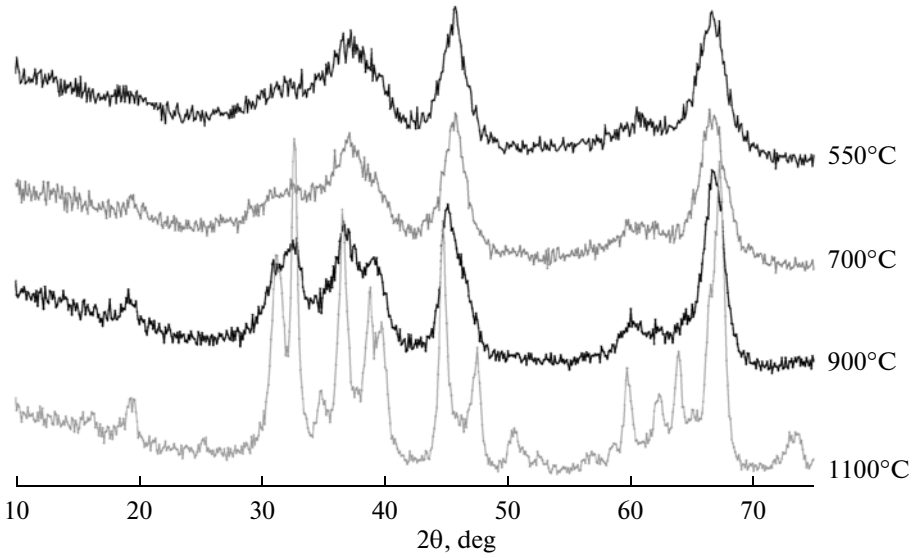

Fig. 6. Diffraction curves of sample A-8 calcined at different temperatures.

Sample A-7 calcined at 300°C consisted of particles shaped as distorted needles, which had the same sizes as the needles in the sample dried at 110°C, namely, a length of 50–150 nm and a width of 7–20 nm (Fig. 4a). The TEM images show that the particle structure in this sample became defective. This manifested itself as the loosening of particle surfaces, the appearance of mesopores in the bulk of the particles, and the partial amorphization of the structure (Fig. 4b). The oxidation of PVA on the surface of the particles after the treatment of the sample at 300°C can be responsible for the appearance of defects in the sample. The high-resolution TEM image shows the disordered structure of Al_2O_3 near the particle edge (Fig. 4b). The EDX spectra suggest the presence of carbon in the needles in an amount that corresponds to the atomic ratio C : Al ≈ 10 : 90 (Fig. 4c). It is likely that carbon in an amorphous form is localized in the above disordered layer on the surface of Al_2O_3 needles. Note that the specific surface area of the sample (545 m^2/g) was greater than the initial S_{BET} = 125 m^2/g; this is consistent with changes in the morphology and structure of aluminum oxide particles.

Figure 5 shows the diffuse reflectance spectra of sample A-7 calcined at different temperatures. The spectrum of the sample obtained in the presence of PVA and dried at 110°C (spectrum *1*) exhibited an intense absorption band at 195–230 nm. Because there are no absorption bands in the region above 170 nm in the spectrum of PVA, it is believed that PVA

Table 3. Phase composition and structure characteristics of sample A-8 calcined at different temperatures

Calcination temperature, °C	Phase composition		
	phase	a, Å	CSD, Å
550	γ-Al_2O_3	7.933	40
700	γ-Al_2O_3	7.927	45
900	δ-Al_2O_3	–	80–100
1100	θ-Al_2O_3	–	155

Table 4. Texture characteristics of samples calcined at 550°C

Sample	Texture characteristics		
	S_{BET}, m^2/g	V_{pore}, cm^3/g	D_{mean}, Å
A-1	315	0.50	64
A-2	365	0.57	63
A-3	325	0.46	56
A-4	345	0.50	58
A-5	455	0.71	62
A-6	490	1.01	82
A-7	500	1.71	137
A-8	495	1.04	84
A-9	530	1.40	105
A-10	250	1.20	192

underwent partial decomposition with the formation of unsaturated carbonyl compounds upon the interaction of the alcohol with the surface of aluminum hydroxide [16]. The observed absorption bands can be assigned to the $\pi \rightarrow \pi^*$ transition in unsaturated oxygen-containing compounds. In the spectrum of Al_2O_3 obtained in the presence of PVA and calcined at 300°C (spectrum *2*), a broad intense absorption band was observed in the region of 300–720 nm, which may be indicative of the formation of polyene coke on the sample surface during PVA dehydration [18]. The spectra of the sample of Al_2O_3 obtained in the presence of PVA and calcined at 550°C (spectrum *3*) and aluminum oxide prepared by a traditional method without a surfactant (spectrum *4*) are similar, except for the fact that spectrum *3* contains a broad absorption band at 700 nm. This absorption band was likely due to the $S_1^*-S_0$ or $T-S_0$ electron transitions in polycyclic aromatic hydrocarbons [19]. This may be indicative of the presence of condensed coke on the surface of the sample.

Thus, according to diffuse reflectance spectroscopic data, the sample obtained in the presence of PVA and calcined at 300°C was covered with polyene coke, which increased the specific surface area of aluminum oxide. Raising the treatment temperature to 550°C led to the formation of not only a better crystallized γ form but also condensed aromatic coke, in the presence of which the specific surface area of the oxide remained sufficiently high.

Sample A-8, which was synthesized with the use of 10% PVA and was aged for 120 h at 110°C, was calcined at 550, 700, 900, and 1100°C. Figure 6 shows the diffraction patterns of this sample, and Table 3 specifies its phase composition.

According to X-ray diffraction data (Table 3), sample A-8 calcined at 550°C was γ-Al_2O_3 with the unit cell parameter $a = 7.933$ Å and a CSD size of 40 Å. Consequently, an increase in the time of aging from 24 h (sample A-7) to 120 h (sample A-8) had almost no effect on the oxide structure (the parameter a for these samples was the same); only an insignificant increase in the size of crystallites from 30 to 40 Å was observed. As the thermal treatment temperature was increased to 700°C, the unit cell parameter of γ-Al_2O_3 increased to 7.927 Å and the crystallite size increased to 45 Å. The sample calcined at 900°C was incompletely formed δ-aluminum oxide with CSD of 80–100 Å. It was very difficult to measure the unit cell parameters and to more accurately determine the sizes of CSDs because of the significant overlapping of diffraction peaks. Sample A-8 calcined at 1100°C was θ-Al_2O_3 with a crystallite size of 155 Å. This surprising result suggests that the presence of PVA at the hydroxide synthesis stage continued to exert a stabilizing effect on the size of oxide crystallites even at high treatment temperatures. This should also be reflected specific surface area data.

Indeed, use of a surfactant and the variation of synthesis conditions influenced the specific surface area, the mean pore diameter, and the pore volume of aluminum oxides obtained at 550°C. According to data obtained by the low-temperature adsorption of nitrogen (Table 4), the specific surface areas of the majority of samples prepared in the presence of surfactants were greater than the S_{BET} of sample A-1 synthesized without surfactants.

The specific surface area of sample A-2 containing 40 wt % CTAB and calcined at 550°C, was approximately 50 m^2/g greater than that of sample A-1. The pore volume and the mean pore diameter remained almost unchanged (Table 4). An increase in the aging temperature and time of sample A-5, which contained 40% CTAB, to 110°C and 72 h, respectively, led to an increase in the specific surface area by 90 m^2/g; simultaneously, the pore volume somewhat increased (to 0.7 cm^3/g), whereas the mean pore diameter remained unchanged (Table 4).

Use of 40% PVA for the preparation of sample A-3 under conditions analogous to the synthesis conditions of sample A-1 did not cause significant changes

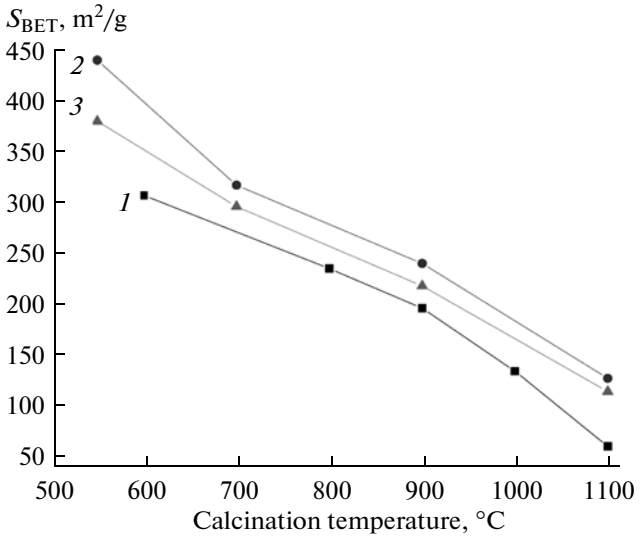

Fig. 7. Dependence of the specific surface area of aluminum oxide samples on calcination temperature: (*1*) a sample with no surfactant, (*2*) a sample containing 10% PVA, and (*3*) a sample containing 40% PVA.

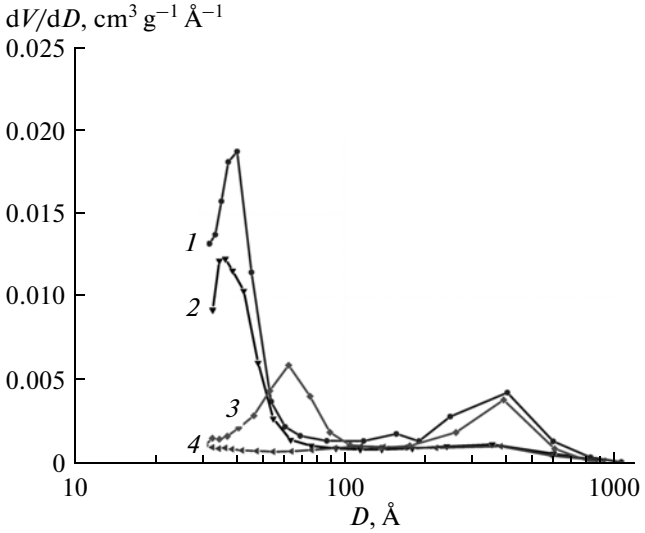

Fig. 8. Pose size distribution in sample A-6 calcined at temperatures of (*1*) 550, (*2*) 700, (*3*) 900, and (*4*) 1100°C.

in the texture characteristics of the oxide calcined at 550°C. At the same time, the specific surface area of sample A-6 increased by more than 150 m^2/g as the aging temperature and time were increased to 110°C and 72 h, respectively, as compared with sample A-3 (to 490 m^2/g), and the pore volume increased by a factor of 2 (to 1 cm^3/g). The mean pore diameter changed to a lesser degree: from 56 Å in sample A-3 to 82 Å in sample A-6 (Table 4).

A decrease in the fraction of PVA to 10% in the synthesis of aluminum hydroxide makes it possible to improve the texture characteristics of aluminum oxide calcined at 550°C: sample A-7, aged at 110°C for 24 h, was characterized by S_{BET} = 500 m^2/g, V_{pore} = 1.7 cm^3/g, and the mean pore diameter D = 137 Å (Table 4). An increase in the aging time to 120 h (sample A-8) did not change the specific surface area (Table 4), but it decreased the volume and the mean pore diameter to 1.0 cm^3/g and 84 Å, respectively. In turn, a decrease in aging temperature and time to 70°C and 3 h, respectively (sample A-9), made it possible to obtain aluminum oxide with the greatest specific surface area of 530 m^2/g (Table 4), a pore volume of 1.4 cm^3/g, and a mean pore diameter of 105 Å. However, as the precipitation temperature was increased from 30 to 70°C under the same aging conditions (70°C, 3 h), the specific surface area sharply decreased to 250 m^2/g (sample A-10 in Table 4), the pore volume decreased to 1.2 cm^3/g, and the mean pore diameter increased by a factor of about 2 to reach 190 Å.

Thus, the introduction of surfactants at the aluminum hydroxide synthesis stage and the variation of aging conditions make possible to obtain γ-aluminum oxide after thermal treatment at 550°C; this aluminum oxide was characterized by a higher specific surface area, pore volume, and mean pore diameter. It is better to use PVA as a pore-forming agent because it more effectively affects the formation of the texture of aluminum oxide even at a lower surfactant concentration; moreover, it is less expensive than CTAB.

The dependence of the texture characteristics of samples on the temperature of their treatment is also of considerable interest. For this reason, samples A-6 and A-8 (Table 1) with different PVA concentrations in a suspension (40 and 10 wt %) and different aging times (72 and 120 h, respectively) were calcined in a muffle furnace at 700, 900, and 1100°C, and the texture characteristics of the resulting oxides were compared. It turned out that the calcined oxides exhibited

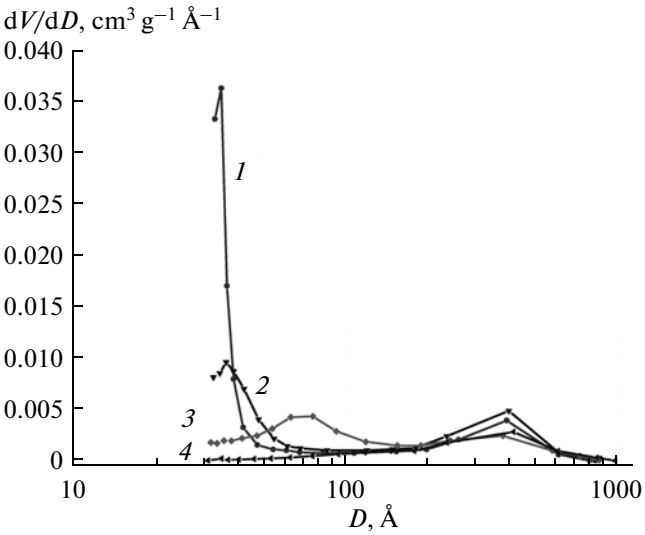

Fig. 9. Pose size distribution in sample A-8 calcined at temperatures of (*1*) 550, (*2*) 700, (*3*) 900, and (*4*) 1100°C.

Table 5. Texture characteristics of samples A-6 and A-8 calcined at 550–1100°C in a muffle furnace

Sample	Calcination temperature, °C	Texture characteristics		
		S_{BET}, m^2/g	V_{pore}, cm^3/g	D_{mean}, Å
A-6	550	380	1.98	209
	700	296	0.86	116
	900	218	1.48	271
	1100	114	0.58	205
A-8	550	440	1.61	147
	700	317	1.78	225
	900	240	1.32	220
	1100	127	1.15	365

a higher thermal stability compared to the sample containing no surfactant (Fig. 7). The specific surface areas of samples A-6 and A-8 in the temperature range of 550–1100°C were 50–100 m^2/g higher than that of sample A-1. After calcination at 1100°C, samples A-6 and A-8 exhibited specific surface areas of 114 and 127 m^2/g, pore volumes of 0.6 and 1.15 cm^3/g, and mean pore diameters of 365 and 205 Å, respectively (Table 5). The results shown in Figs. 8 and 9 indicate that the pore size distributions in samples A-6 and A-8 were mainly bimodal with maximums in the ranges of 35–65 and 380–415 Å. Note that a high PVA content (40%) in the synthesis of sample A-6 led to a strong decrease in the specific surface area, the total pore volume, and the mean pore diameter at temperatures of 700–1100°C (Table 5, Fig. 7).

Thus, this study demonstrated that the introduction of different surfactants at different concentrations at the stage of the precipitation of aluminum hydroxide makes it possible to regulate the textural characteristics of aluminum oxide in wide ranges: the specific surface area, pore volume, and mean pore diameter can vary from 125 to 545 m^2/g, from 0.5 to 2.0 cm^3/g, and from 56 to 365 Å, respectively.

ACKNOWLEDGMENTS

We are grateful to T.Ya. Efimenko for measuring the texture characteristics of the samples.

This work was supported by the Ministry of Education and Science of the Russian Federation (contract no. 14.740.11.0419).

REFERENCES

1. Antonelli, D.M. and Ying, J.Y., *Angew. Chem. Int. Ed.*, 1995, vol. 34, p. 2014.
2. Ciesla, U., Schacht, S., Stucky, G.D., Unger, K.K., and Schüth, F., *Angew. Chem. Int. Ed.*, 1996, vol. 35, p. 541.
3. Balint, I. and Miyazaki, A., *Microporous Mesoporous Mater.*, 2009, vol. 122, p. 216.
4. Bai, P., Wu, P., Yan, Z., and Zhao, X.S., *Microporous Mesoporous Mater.*, 2009, vol. 118, p. 288.
5. Huo, Q., Margolese, D.I., Ciesla, U., Demuth, D.G., Feng, P., Gier, T.E., Sieger, P., Firouzi, A., Chmelka, B.F., Schüth, F., and Stucky, G.D., *Chem. Mater.*, 1994, vol. 6, p. 1176.
6. Yada, M., Machida, M., and Kijima, T., *J. Chem. Soc., Chem. Commun.*, 1996, p. 769.
7. Yada, M., Hiyoshi, H., Ohe, K., Machida, M., and Kijima, T., *Inorg. Chem.*, 1997, vol. 36, p. 5565.
8. Valange, S., Guth, J.-L., Kolenda, F., Lacombe, S., and Gabelica, Z., *Micropor. Mesopor. Materials*, 2000, vol. 35–36, p. 597.
9. Aguado, J., Escola, J.M., and Castro, M.C., *Microporous Mesoporous Mater.*, 2010, vol. 128, p. 48.
10. Lesaint, C., Kleppa, G., Arla, D., Glomm, W.R., and Oye, G., *Microporous Mesoporous Mater.*, 2009, vol. 119, p. 245.
11. Boehm, H.-P. and Knozinger, H., in *Catalysis Science and Technology*, Anderson, J.R. and Boudart, M., Eds., Berlin: Springer, 1983, vol. 4, p. 39.
12. Ivanova, A.S., Litvak, G.S., Kryukova, G.N., Tsybulya, S.V., and Paukshtis, E.A., *Kinet. Catal.*, 2000, vol. 41, no. 1, p. 122.
13. Joo Hyun Kim, Kyeong Youl Jung, Kyun Young Park, and Sung Baek Cho, *Microporous Mesoporous Mater.*, 2010, vol. 128, p. 85.
14. Ivanova, A.S., Litvak, G.S., Moroz, E.M., Kryukova, G.N., and Malakhov, V.V., *Izv. Sib. Otd. Akad. Nauk SSSR, Ser. Khim. Nauk*, 1990, no. 5, p. 62.
15. Ushakov, S.N., *Polivinilovyi spirt i ego proizvodnye* (Polyvinyl Alcohol and Its Derivatives), Moscow: Akad. Nauk SSSR, 1960, vols. 1, 2.
16. Rozenberg, M.E., *Polimery na osnove polivinilatsetata* (Polyvinyl Acetate–Based Polymers), Leningrad: Khimiya, 1983,.
17. Ushakov, V.A., Moroz, E.M., and Levitskii, E.A., *Kinet. Katal.*, 1985, vol. 26, p. 1200.
18. Berlin, A.A., Geiderikh, M.A., Davydov, B.E., Kargin, V.A., Karpacheva, G.P., Krentsel', B.A., and Khurareva, G.V., *Khimiya polisopryazhennykh sistem* (Chemistry of Polyconjugated Systems), Moscow: Khimiya, 1972.
19. Nurmukhametov, R.N., *Pogloshchenie i lyuministsentsiya aromaticheskikh soedinenii* (Light Absorption and Luminescence of Aromatic Compounds), Moscow: Khimiya, 1971.